NIH Public Access
Author Manuscript
Methods. Author manuscript; available in PMC 2010 March 1.

Published in final edited form as:
Methods. 2009 March ; 47(3): 214–222. doi:10.1016/j.ymeth.2008.10.022.

Structure and dynamics of single DNA molecules manipulated by magnetic tweezers and or flow

Sanford H. Leuba[a,*], **Travis B. Wheeler**[a], **Chao-Min Cheng**[b], **Philip R. LeDuc**[b], **Mónica Fernández-Sierra**[c], and **Edwin Quiñones**[c]

[a] Departments of Cell Biology and Physiology and Bioengineering, University of Pittsburgh School of Medicine and Swanson School of Engineering, Petersen Institute of NanoScience and Engineering and University of Pittsburgh Cancer Institute, Hillman Cancer Center, Pittsburgh, Pennsylvania 15213, USA

[b] Departments of Mechanical and Biomedical Engineering and Biological Sciences, Carnegie Mellon University, Pittsburgh, Pennsylvania 15213, USA

[c] Department of Chemistry, University of Puerto Rico, Río Piedras Campus, P.O. Box 23346, San Juan, Puerto Rico 00931, USA

Abstract

Here we describe experiments which employ magnetic tweezers and or microfluidics to manipulate single DNA molecules. We describe the use of magnetic tweezers coupled to an inverted microscope as well as the use of a magnetic tweezers setup with an upright microscope. Using a chamber prepared via soft lithography, we also describe a microfluidic device for the manipulation of individual DNA molecules. Finally, we present some past successful examples of using these approaches to elucidate unique information about protein-nucleic acid interactions.

Keywords

magnetic tweezers; single DNA molecules; soft lithography microfabrication; micro- and nanofluidic approaches; single DNA manipulation

1. Introduction

Magnetic tweezers instrumentation has been used extensively to manipulate individual DNA molecules (reviewed in [1]). Essentially, the magnetic tweezers setup used to study the behavior of individual nucleic acids is an optical microscope combined with a magnetic field to mechanically manipulate individual linear DNA molecules. A magnetic field is created with one or more permanent- or electro-magnets. A wide diversity of studies have been accomplished using this approach, such as tethering the DNA at both ends between a glass surface and a superparamagnetic bead and then pulling the bead by applying magnetic fields. The simplicity of these kinds of instruments makes them relatively accessible for researchers

*Contact information: Sanford H. Leuba, Ph.D., 2.26g Hillman Cancer Center, 5117 Centre Avenue, Pittsburgh, PA 15213-1863 USA, Telephone: +1 412-623-7788, Fax: +1 412-623-4840, E-mail: leuba@pitt.edu.

Publisher's Disclaimer: This is a PDF file of an unedited manuscript that has been accepted for publication. As a service to our customers we are providing this early version of the manuscript. The manuscript will undergo copyediting, typesetting, and review of the resulting proof before it is published in its final citable form. Please note that during the production process errors may be discovered which could affect the content, and all legal disclaimers that apply to the journal pertain.

NIH-PA Author Manuscript
NIH-PA Author Manuscript
NIH-PA Author Manuscript

NIH-PA Author Manuscript

NIH-PA Author Manuscript

NIH-PA Author Manuscript

studying processive nucleic acid motor proteins as well as proteins that create loops in nucleic acids.

The use of microfluidics (reviewed in [2,3]) to manipulate individual DNA molecules is perhaps less well known in the nucleic acid research field. Through the use of microfluidic approaches, researchers can design and construct flow chambers with dimensions down to the single micron and even sub-micron range. The use of materials such as polydimethylsiloxane (PDMS) allows the researcher to reproducibly and inexpensively construct these microscale flow chambers. These microfluidic devices are able to control the properties of molecules of DNA using flow conditions while probing the response with other novel integrated assays. For example, microfluidic-based approaches have been used to place specific kinds of forces on a linear nucleic acid tethered to a surface and to differentiate different lengths of untethered nucleic acids via their different mobilities while undergoing electrophoresis through microns-sized obstacles.

2. Magnetic tweezers instrumentation

We and others have described versions of magnetic tweezers used to manipulate individual molecules of DNA (e.g., [4–14]).

2.1 Magnetic tweezers instrumentation construction

Typically, magnetic tweezers have been constructed using an inverted microscope which allows for an extensive amount of space above the objective for placing the external permanent- or electro-magnets. We present such a setup here (Fig. 1a) and an example of the manipulation of a magnetic bead decorated with a smaller bead by controlling the rotation of the external magnets (Fig. 1b–g). It is also possible to setup an upright microscope with magnetic tweezers (schematic in Fig. 1i and photo in Fig. 1o). Typically, because the condenser lens is right next to the objective in such a microscope, there is insufficient space to place the magnets below the stage. Using a ball bearing with inner diameter larger than the objective itself allows for a MT to be built around the objective (photos in Figs. 1l, m and o). To the suspended ball bearing are attached the permanent magnets (Fig. 1l). In addition to magnetic tweezers built with inverted and upright microscopes, the MT can also be setup horizontally with an objective mounted on a three-axis flexure stage, as we have previously described [10].

Three different flow cells are presented in this article. One flow cell is made from soft lithography using Polydimethylsiloxane. Another flow cell is described in protocol 3.4 (Fig. 1h, p). Finally, it is also possible to use commercial rectangular flow cuvettes (VitroCom) to increase the throughput of experiments. We have previously described methods for using a 1 mm × 1 mm × 50 mm square glass cuvette [10]. However, the distance between the two inside surfaces is typically greater than the working distances of high-powered objectives, and it is easy to obtain distorted views of the superparamagnetic beads with such cuvettes. The rounded corners of the cuvettes also distort images when viewed too close at an edge, which is relatively easy to do because the 1 mm width is relatively narrow for an objective. VitroCom also manufactures flat, rectangular microslides of dimensions 0.2 mm × 2 mm inner diameter × 100 mm long (Cat. # 3520-100). Because these cuvettes are 2 mm wide rather than 1 mm wide, they offer flat fields of view for the objective. The narrow 0.2 mm thickness is typically within the working distances of most objectives, and the long 100 mm length allows a large area for examination using a microscope stage. The glass in these cuvettes is thick enough to allow connection via silicon tubing (BioRad 1.6 mm ID silicon tubing, Cat. # 731–8211) with a minimal amount of parafilm required for complete sealing.

NIH-PA Author Manuscript

NIH-PA Author Manuscript

NIH-PA Author Manuscript

2.2 MT machining

The microslide holder (photographs in Fig. 1n and o and schematics in Figs. 2 and 3) was machined from black acetal/delrin that measured 190 mm long × 102 mm wide × 25.4 mm high for the base (Figs. 2 and 3). The system was designed using AutoCAD software and machined using Feature Cam software on a Bridgeport 3 Axis CNC. Though computer software was used, some of the machining processes were still done using manual machining methods. Most of the machining was done with a 9-mm endmill but other tooling to include slitting saws, drills and taps were employed as well. The unit was designed and built in a manner that will allow for future modifications and upgrades for the changing scientific arena.

3. Preparation of DNA construct, immobilization surface, superparamagnetic microspheres and flow cell

In order to immobilize and manipulate the DNA molecules, we followed previously published procedures [9,14] to prepare a λ-DNA construct with a biotin molecule attached to one end and a magnetic microsphere on the other (Fig. 4a).

3.1 DNA construct

The following oligonucleotides were used to create the construct: GGG CGG CGA CCT AAA AAA AAA AAA AAA AAA AAA AA-3′ Biotin, 5′ Digoxigenin-AAA AAA AAA AAA GGC TGC TCC TGC, and a linker with the sequence AGG TCG CCG CCC GCA GGA GCA GCC. The 5′-ends of the λ-DNA and oligonucleotides were phosphorylated using T4 polynucleotide kinase at 37°C in an ATP-containing buffer (50 mM Tris-HCl, pH 7.5, 10 mM $MgCl_2$, 1 mM ATP, 10 mM Dithiothreitol, 25 μg/ml BSA). The biotin-modified oligonucleotide was annealed first, followed by the linker and the digoxigenin end. Before each annealing step, an excess of the oligonucleotide was mixed with the phosphorylated λ-DNA and heated to 65°C to ensure that the sticky ends are in single-stranded form. The annealing of each oligonucleotide was achieved by incubation with T4 DNA ligase at room temperature, with an excess amount of the oligonucleotide. All enzymes and λ-DNA were purchased from New England Biolabs (Ipswich, MA). Custom oligonucleotides were purchased from Integrated DNA Technologies (Coralville, IA).

3.2 Coverslip surface modification

Glass coverslips are covalently modified to bind the DNA construct molecules via biotin-streptavidin attachment chemistry (Fig. 4b). First, amino groups are introduced to the coverslip surface by incubation with 2% v/v (3-Aminopropyl)triethoxysilane (APTES) in acetone during 5 minutes, followed by rinsing with excess water to stop the reaction. The coverslips are then cured in an oven for 30 minutes at 110 °C. After cooling down, the dry coverslips are treated with 1 mg/ml biotin-PEO_4-NHS (Pierce Biotechnology) in 100 mM sodium bicarbonate buffer (pH 8.3). The reaction is allowed to occur for at least 3 hours, after which the coverslips are rinsed with water and dried with air. The biotinylated surface is then treated with 200 μg/ml streptavidin for 30 minutes, followed by rinsing with water and drying with nitrogen.

3.3 Functionalization of superparamagnetic microspheres

Carboxy-modified superparamagnetic microspheres (Dynabeads M-270 carboxylic acid, 2.8 μm) are coated with anti-digoxigenin antibody (Fig. 4c) for specific binding to the digoxigenin-modified end of the DNA construct. The spheres are first washed with 10 mM NaOH, followed by three washes with nanopure water. Then the microspheres are reacted with EDC and NHS in MES, pH 5.0, mixing slowly for 30 minutes at 22 °C. This is done inside a dry box to avoid hydrolysis of the reagents. Subsequently, the spheres are washed with 25 mM MES and then three times with 100 mM carbonate buffer, pH 8.0. A 2.5 mg/ml solution of anti-digoxigenin

NIH-PA Author Manuscript

NIH-PA Author Manuscript

NIH-PA Author Manuscript

(Fab fragments from sheep, Roche Applied Science) in carbonate buffer, pH 8.0, is added to the spheres, and the reaction is slowly mixed for two hours at 0 °C. Non-reacted carboxylic acid groups can be quenched by incubating the microspheres with 50 mM Tris-HCl, pH 8.0, mixing slowly for 30 minutes at room temperature.

3.4 Flow cell preparation

The first generation flow cell (Fig. 1h) is based on the design created by the research group of Dr. A. van Oijen [9]. We have subsequently adapted the original design to include several channels on each flow cell, thus allowing us to carry out several experiments on each glass substrate (Fig. 1p). The bottom of the flow cell is a 2.2 cm × 5.0 cm glass coverslip with a thickness of 0.13 –0.17 mm. The top of the flow cell consists of a 2.5 cm × 7.5 cm glass slide in which we drill holes of 1.5 mm diameter each. The flow channels are created using double-sided adhesive tape as a spacer between the coverslip and the slide, and carving approximately 0.8 mm-wide channels between each pair of holes. If a constant flow is required, two flexible clear PVC tubes with an external diameter of 1.5 mm can be inserted into the holes to be used as inlet and outlet, sealing the connections with epoxy glue. These microcells are appropriate to be used with an inverted microscope. A magnet or microflow can be used to stretch the immobilized DNA molecules in order to study reactions at the single-molecule level.

3.5 Kinetics of lambda exonuclease

The lambda DNA construct described above and tethered to a superparamagnetic microsphere has been employed as a substrate to study reactions of lambda exonuclease, which has 5′ to 3′ polarity [15,16,9]. Lambda exonuclease loads itself as a trimeric quaternary structure onto a single-stranded region of the DNA molecule. Performing an essential step in homologous recombination, this prokaryotic enzyme continuously excises nucleotides from one end of the DNA strand, generating single-stranded segments [17]. To study this class of reactions, it is necessary to stretch the biopolymer, which can be accomplished by applying a magnetic force in the range of 1 to 5 pN. When forces of this magnitude act on the DNA molecule it is observed that the single-stranded segments tend to form secondary structures (e.g., hairpins) making them shorter than double-stranded ones. In the experimental scheme of Xie and co-workers, the enzyme moves using one of the strands as a track [9]. Perkins et al. utilized a different approach by attaching the enzyme to the surface of a microsphere and following the motion of the bead as one strand was digested [16].

Since the microspheres attached to DNA are opaque, they are observed as dark circles under the microscope when they are illuminated from above the stage, which means the DNA molecules are not observed directly. A simple way to measure the contour length of the biopolymer is to apply a hydrodynamic force, then invert the flow direction and measure the position of the bead again. The total displacement of the sphere will be two times the length of the DNA molecule plus the diameter of the microsphere (assuming that the computer program employed searches for the center of the sphere to assign its coordinates). This procedure also allows the determination of the position at which the DNA molecules are bound to the surface of the coverslip. To validate the procedure just described, it is advisable to construct an extension-force curve to compare it with those previously described in the literature. Once the reaction is initiated, the length of the DNA molecule decreases with time (the microsphere moves towards the point it is attached on the surface), and this is the key concept to study this class of reactions.

It is important to maintain a constant tension on the DNA molecule during the reaction. Here we describe a method widely used to measure this force. To this end, we have used the model of an inverted pendulum [7] in which the bob is the microsphere and the string is the length L of the DNA molecule. In the case of the λ DNA molecule, $L \approx 16.4\ \mu$m. The oscillations of

NIH-PA Author Manuscript

NIH-PA Author Manuscript

NIH-PA Author Manuscript

the bead are caused by thermal fluctuations, and the restoration force is one of the components of the applied magnetic force. Before starting the reaction, one must record the Brownian motion of the microsphere for a few seconds using a video camera. To accurately determine the mean-square displacement, it is important to wait long enough to allow the microsphere to span the whole phase space. The videos may be analyzed frame-by-frame using a commercial computer program (e.g., MaxTRAQ) to calculate the variance of the displacement, $\langle \delta x^2 \rangle$, in the coordinate perpendicular to the DNA axis, which by definition coincides with the *z*-axis. This information along with the equipartition theorem permits the determination of the magnitude of the tension on the DNA, $\langle F \rangle = k_B TL/\langle \delta x^2 \rangle$, where k_B is the Boltzmann constant and T is the temperature in Kelvin. Once the reaction is initiated, videos are recorded to follow the position of the microsphere as a function of time during the reaction. If the zero-time of the reaction needs to be defined precisely this can accomplished by adding first the enzyme, waiting until it is loaded [18] and then adding the magnesium ion co-factor when the experimenter is ready to initiate the reaction.

The shortening of the DNA molecule as a function of time may be related to the motion of the enzyme along the DNA molecule through a simple algebraic equation. In addition, if the DNA molecule is not stretched parallel to the coverslip surface it is necessary to include a geometric factor to obtain L at an arbitrary reaction time because the microscope detects the projection of L in the plane parallel to the surface of the coverslip.

Two advantages of the experimental designs we have been describing over conventional techniques are that the method allows (1) studying reactions in real-time as well as (2) monitoring the progress of the reaction of one enzyme molecule at a time. This level of sophistication greatly reduces the problems of interpretation created by ensemble averaging. In our opinion, single molecule measurements represent a shift of paradigm in which individual molecules ‘communicate’ information to the experimenter as opposed to the traditional way of performing experiments in which a large group of molecules are interrogated incoherently. This is analogous to the relationship that exists between quantum and classical mechanics. A quantum mechanical operator (e.g., a Hamiltonian operator to calculate the energy of a system) is constructed starting from a classical mechanic one. To confirm if a quantum mechanical operator provides an adequate description of a system, it must satisfy the principle of correspondence, which states that as the quantum numbers approach infinity, the system must start again to obey the laws of classical mechanics. More related to the present discussion, if the reactivity of N identical enzyme molecules is studied at the single-molecule level to calculate the rate constant k_i ($i = 1$ to N) for each of them, then the average value should coincide with the constant calculated from experiments performed under bulk conditions. This approach provides the experimentalist with the opportunity to observe hitherto inaccessible information. In particular, one may observe if the enzyme pauses [16], dissociates [9], changes the rate of nucleotide digestion for different base sequences [19,20], or changes the rate of nucleotide digestion upon applying a stretching force.

4. Soft lithography methods to probe DNA dynamics

Polymer dynamics plays an important role in various research fields such as materials science, physics, biology and medicine. Single polymer dynamics have provided exciting insights in these areas including the understanding of cell structure and structural dynamics in cellular processes. In this field, advances in micro- and nano-scale technologies such as microfluidic and microfabrication systems have been widely used for rapid analysis of biological samples. Here, we discuss various micro- and nanofluidic approaches, which have been used to observe the dynamics of individual flexible polymers (e.g. fluorescently labeled DNA molecules).

NIH-PA Author Manuscript

NIH-PA Author Manuscript

NIH-PA Author Manuscript

We have developed an approach to observe and measure real-time dynamics of individual flexible polymers under a microvortex flow. We first fabricated a microfluidic channel to create a high radial acceleration, which can both stretch and bend individual polymers simultaneously; a schematic of this system is shown in Fig. 5a. This microfluidic device was fabricated using standard soft-lithography methods with poly(dimethylsiloxane); Fig. 5b is a schematic of the soft lithography method. Fig. 5c is an optical image of the microfluidic device. To control the flow velocity in the device for imposing defined radial accelerations on the DNA, we characterized the flow profile by imaging 2 μm in diameter fluorescent beads with epi-fluorescent microscopy. We found that the average linear velocity of the pressure-driven flow in the side chamber increased in proportion to an increase in the applied syringe pump pressure. We also noted that flow response in this environment was different than that observed in a macroscale lid-driven cavity flow. The combination of a tight rotation radius (r <50 μm) and a high rotational velocity (v ~1.75 m/s) for the flow in the constricted channel generated a radial acceleration (v^2/r) as high as 10^5 m/s^2 when the flow rate was 100 μl/min. Figs. 5d and 5e show an individual polymer that was deformed through this microvortex flow at the flow rate of 75 μl/min.

Using another approach that has produced interesting results, Stein *et al.* [21] observed two distinct transport regimes of individual DNA molecules while using a pressure-driven transport of these molecules through silica fluidic channels as shown in Figs. 6a and 6b. The results from these studies include determining polymer transport properties that are of considerable significance to lab-on-a-chip technology aimed at the separation of DNA by length or the uniform transport of DNA molecules through a microfluidic system. To probe these responses, the trajectory of each DNA molecule's center of mass was tracked over a series of images (Fig. 6c). Based on these observations, the pressure-driven mobility of individual DNA molecules was determined to increase with molecular length in channels with dimensions that were multifold higher than the radius of gyration of the molecule. The DNA mobility though was practically independent of molecular length in thin channels. In addition, both the Taylor dispersion and the self-diffusion of DNA molecules decreased significantly in confined channels in accordance with scaling relationships.

The ability to probe fundamental relationships of DNA has been significantly enhanced through using fabrication techniques. Tegenfeldt *et al.* [22] showed that genomic-length DNA molecules imaged in nanochannels have an extension along the channel that scales linearly with the contour length of the polymer as shown in Figs. 7a and 7b. This was in agreement with the scaling arguments developed by de Gennes [23] for self-avoiding confined polymers. This fundamental relationship allowed them to measure directly the contour length of single DNA molecules confined in the channels. In addition, the analysis of the dynamics of the polymer in the nanochannel allowed them to compute the standard deviation of the extension mean.

4.1 Method of soft lithography fabrication

Microfluidic channels are fabricated through the standard soft lithography method. SU-8 photoresist (MicroChem Corp., Newton, MA, USA; Formulations 50–100) is used to create patterns on a silicon wafer, which is implemented as a mold. Polydimethylsiloxane (PDMS; Dow Corning Corp., Midland, MI, USA; No. Sylgard 184) is then cast against this mold to make a microfluidic device that can have various heights and widths. For example, with the microvortex flow, the dimensions of the channels were 30 μm wide and 20 μm deep in the main channel with a circular side chamber. The microfluidic devices are then removed from the mold, and treated with oxygen plasma for at least 1 minute to enhance the bonding to a glass coverslip so that conventional epi-fluorescent microscopy techniques can be implemented.

NIH-PA Author Manuscript

NIH-PA Author Manuscript

NIH-PA Author Manuscript

5. Examples

We present three successful examples of using the described and related procedures to learn more about protein/nucleic acid interactions.

5.1 Visualizing transcription elongation with magnetic tweezers

Fig. 8a is a schematic of a magnetic tweezers experiment to observe transcription elongation. A DNA molecule is tethered between a 2.8 μm superparamagnetic bead and a stalled RNA polymerase. The streptavidin-coated superparamagnetic bead is decorated with a 1 μm biotinylated bead to allow observation of rotation of the superparamagnetic bead. The stalled RNA polymerase is attached to the surface of a glass coverslip, and the DNA tethered to a 2.8 μm bead/1 μm bead assembly is visualized in the video image (Fig. 8b). After the introduction of all four nucleotides sufficient to restart transcription, the marker bead is observed to rotate around the larger bead, evidence that transcription elongation is causing the topologically constrained DNA molecule to rotate the beads [24]. Transcription elongation caused rotation due to an elongating *E. coli* RNA polymerase has also been observed with smaller magnetic beads [25]. Since B-form DNA is 10.2 bp/turn, it should be possible with a fast enough video camera to be able to read the DNA sequence from the rotation as 1 bp should be about a 35 degree rotation.

5.2 Visualizing chromatin assembly and disassembly with magnetic tweezers

We have also used magnetic tweezers to follow the assembly and disassembly of single chromatin fibers [8]. Fig. 9a–d exhibits schematic drawings of video images occurring at various times during the experiment. At the beginning without flow, a tethered superparamagnetic bead is observed in the upper left-hand corner of the video. Upon the introduction of flow, the bead is observed to move to the upper right-hand corner of the video. The flow introduces histone chaperones and core histones, which upon assembly on the tethered DNA molecule reduce the tether length of the DNA molecule and cause the superparamagnetic bead to travel against the flow. At this point, we turn off the flow (Fig. 9e) and follow chromatin assembly as a function of the force exerted by the external magnet on the superparamagnetic bead. We found that we could step-wise adjust the force in a single assembly experiment (Fig. 9f). In addition to what is presented in Fig. 9, we also observed large-scale chromatin rearrangements in realtime during assembly and during disassembly, which is direct evidence of the dynamic nature of chromatin [8].

5.3 Visualizing chromatin assembly with a microfluidic device

Chromatin assembly has been observed with microfluidics [26]. In these experiments, one end of a fluorescently-labeled, linear λ-DNA molecule was tethered to a surface (Fig. 10a). A syringe pump introduced egg extract, and the researchers observed a reduction in length of the λ-DNA molecule over time (Fig. 10b). They studied the reduction in length of the DNA molecule as a function of dilution of the extract (Fig. 10c) or as a function of the flow rate (Fig. 10d). Using a relationship for assembly where the H3/H4 tetramer first assembles on the DNA molecule followed by subsequent assembly of two H2A/H2B dimers, the authors modeled the reaction to identify a subsequent parameter of the DNA/octamers complex to form a nucleosomal core particle [26]. More recently, this same group has torsionally manipulated individual chromatin fibers using magnetic tweezers [27,28].

6. Summary

We hope that presentation of these methods for various forms of magnetic tweezers, flow systems as well as soft lithography fabrication will be of interest and stimulate the reader to construct his or her own experiments. The examples provided should give the reader possibility

NIH-PA Author Manuscript

NIH-PA Author Manuscript

NIH-PA Author Manuscript

of avenues to pursue and techniques that can be implemented in their own labs. The methods that we have presented are not mutually exclusive, and researchers are beginning to combine them (e.g., [29]).

Acknowledgments

We would like to thank Dr. A. van Oijen for extensive advice on the protocols of surface treatment, DNA preparation and functionalization of superparamagnetic microspheres. Supported by National Institutes of Health RO1GM077872 (S.H.L.).

Abbreviations

APTES
(3-Aminopropyl)triethoxysilane

EDC
N-(3-Dimethylaminopropyl)-N′-ethylcarbodiimide

MES
2-(N-morpholino)ethanesulfonic acid

MT
magnetic tweezers

NHS
N-Hydroxysuccinimide

PDMS
Polydimethylsiloxane

References

1. Zlatanova J, Leuba SH. Biochem Cell Biol 2003;81:151–159. [PubMed: 12897848]
2. Larson JW, Yantz GR, Zhong Q, Charnas R, D'Antoni CM, Gallo MV, Gillis KA, Neely LA, Phillips KM, Wong GG, Gullans SR, Gilmanshin R. Lab Chip 2006;6:1187–1199. [PubMed: 16929398]
3. Brewer LR, Bianco PR. Nat Methods 2008;5:517–525. [PubMed: 18511919]
4. Smith SB, Finzi L, Bustamante C. Science 1992;258:1122–1126. [PubMed: 1439819]
5. Strick TR, Allemand JF, Bensimon D, Bensimon A, Croquette V. Science 1996;271:1835–1837. [PubMed: 8596951]
6. Strick TR, Allemand JF, Croquette V, Bensimon D. J Stat Phys 1998;93:647–672.
7. Gosse C, Croquette V. Biophys J 2002;82:3314–3329. [PubMed: 12023254]
8. Leuba SH, Karymov MA, Tomschik M, Ramjit R, Smith P, Zlatanova J. Proc Natl Acad Sci USA 2003;100:495–500. [PubMed: 12522259]
9. van Oijen AM, Blainey PC, Crampton DJ, Richardson CC, Ellenberger T, Xie XS. Science 2003;301:1235–1238. [PubMed: 12947199]
10. Leuba SH, Bennink ML, Zlatanova J. Methods Enzymol 2004;376:73–105. [PubMed: 14975300]
11. Yan J, Skoko D, Marko JF. Phys Rev E Stat Nonlin Soft Matter Phys 2004;70:011905. [PubMed: 15324086]
12. Claudet C, Bednar J. Appl Opt 2005;44:3454–3457. [PubMed: 16007842]
13. Revyakin A, Ebright RH, Strick TR. Nat Methods 2005;2:127–138. [PubMed: 16156080]
14. Kim S, Blainey PC, Schroeder CM, Xie XS. Nat Methods 2007;4:397–399. [PubMed: 17435763]
15. Dapprich J. Cytometry 1999;36:163–168. [PubMed: 10404963]
16. Perkins TT, Dalal RV, Mitsis PG, Block SM. Science 2003;301:1914–1918. [PubMed: 12947034]

NIH-PA Author Manuscript

NIH-PA Author Manuscript

NIH-PA Author Manuscript

17. Subramanian K, Rutvisuttinunt W, Scott W, Myers RS. Nucleic Acids Res 2003;31:1585–1596. [PubMed: 12626699]
18. Mitsis PG, Kwagh JG. Nucleic Acids Res 1999;27:3057–3063. [PubMed: 10454600]
19. Werner JH, Cai H, Keller RA, Goodwin PM. Biophys J 2005;88:1403–1412. [PubMed: 15542563]
20. Enderlein J. Biophys J 2007;92:1556–1558. [PubMed: 17142274]
21. Stein D, van der Heyden FH, Koopmans WJ, Dekker C. Proc Natl Acad Sci USA 2006;103:15853–15858. [PubMed: 17047033]
22. Tegenfeldt JO, Prinz C, Cao H, Chou S, Reisner WW, Riehn R, Wang YM, Cox EC, Sturm JC, Silberzan P, Austin RH. Proc Natl Acad Sci USA 2004;101:10979–10983. [PubMed: 15252203]
23. de Gennes, PG. Scaling Concepts in Polymer Physics. Cornell University Press; Ithaca: 1979.
24. Pomerantz RT, Ramjit R, Gueroui Z, Place C, Anikin M, Leuba S, Zlatanova J, McAllister WT. Nano Lett 2005;5:1698–1703. [PubMed: 16159208]
25. Harada Y, Ohara O, Takatsuki A, Itoh H, Shimamoto N, Kinosita K Jr. Nature 2001;409:113–115. [PubMed: 11343125]
26. Ladoux B, Quivy JP, Doyle P, du Roure O, Almouzni G, Viovy JL. Proc Natl Acad Sci USA 2000;97:14251–14256. [PubMed: 11114182]
27. Bancaud A, Conde e Silva N, Barbi M, Wagner G, Allemand JF, Mozziconacci J, Lavelle C, Croquette V, Victor JM, Prunell A, Viovy JL. Nat Struct Mol Biol 2006;13:444–450. [PubMed: 16622406]
28. Bancaud A, Wagner G, Conde ESN, Lavelle C, Wong H, Mozziconacci J, Barbi M, Sivolob A, Le Cam E, Mouawad L, Viovy JL, Victor JM, Prunell A. Mol Cell 2007;27:135–147. [PubMed: 17612496]
29. Rondelez Y, Tresset G, Nakashima T, Kato-Yamada Y, Fujita H, Takeuchi S, Noji H. Nature 2005;433:773–777. [PubMed: 15716957]

NIH-PA Author Manuscript

NIH-PA Author Manuscript

NIH-PA Author Manuscript

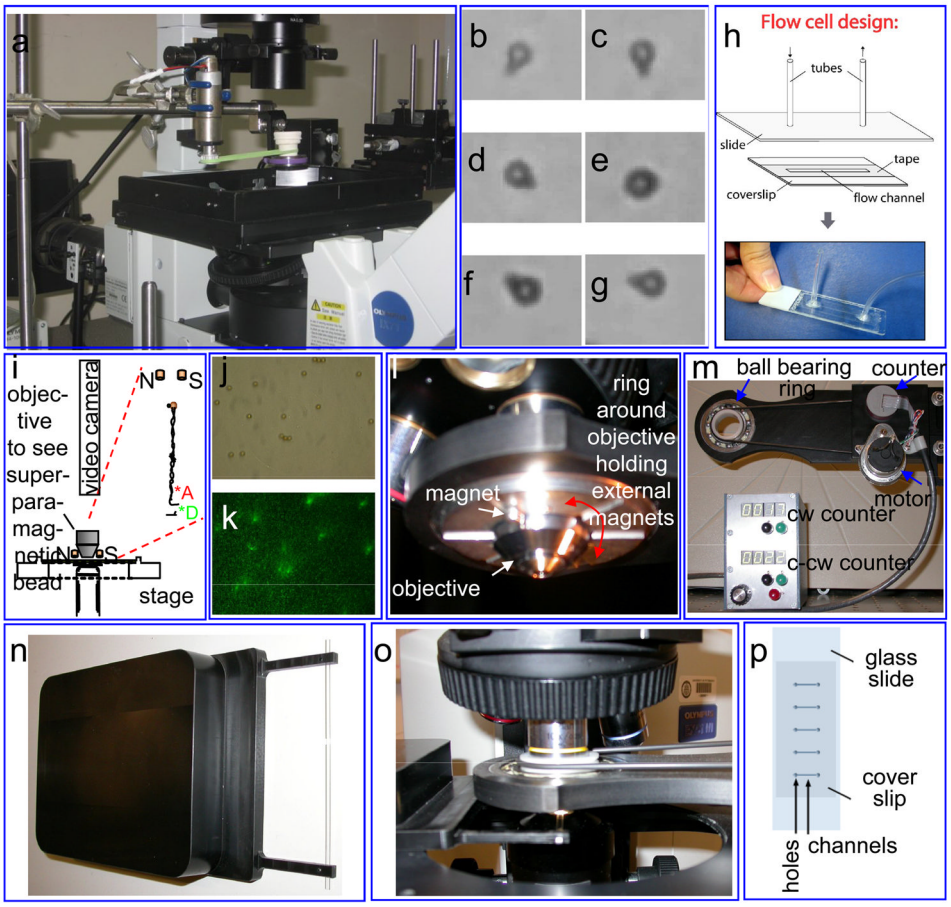

Fig. 1.

Magnetic tweezers (MT).

(a) Photograph of MT system on an inverted microscope with belt driven MT. (b–g) Microscope video images of one bead rotating around a magnetic bead due to the rotation of the external magnets of the belt driven MT in (a). Sequential order of images is b, c, d, e, f and g. (h) Schematic example of first generation flow cell design using parafilm and photograph of assembled flow cell. (i) Schematic of MT operation on an upright microscope with inset of individual DNA molecule suspended between a superparamagnetic bead and the surface. Photograph of same area containing 2.8 μm Dynal superparamagnetic beads attached to the glass slide illuminated by white light (j) or by scatter of a 532 nm laser (k). (l) Photograph of the ring around the objective. This large diameter ring can rotate external magnet(s) clockwise and counter-clockwise around the objective and can be used for the MT setup above the microscope slide. (m) Photograph of the external ring setup portion of MT. Counter, motor, measurement of number of clockwise (cw) and counter cw (c-cw) rotations, and ball bearing ring are indicated. On opposite side of ball bearing is the place for magnets as in (l). (n) Photograph of assembly for holding 0.2 × 2.0 × 100 mm microslide (VitroCom, Cat. # 3520-100) with two buffer reservoirs for attachment to the ends of this rectangular cuvette. (o) Photograph of cuvette holder and MT on an upright microscope. (p) Photograph of second generation flow cell design.

NIH-PA Author Manuscript

NIH-PA Author Manuscript

NIH-PA Author Manuscript

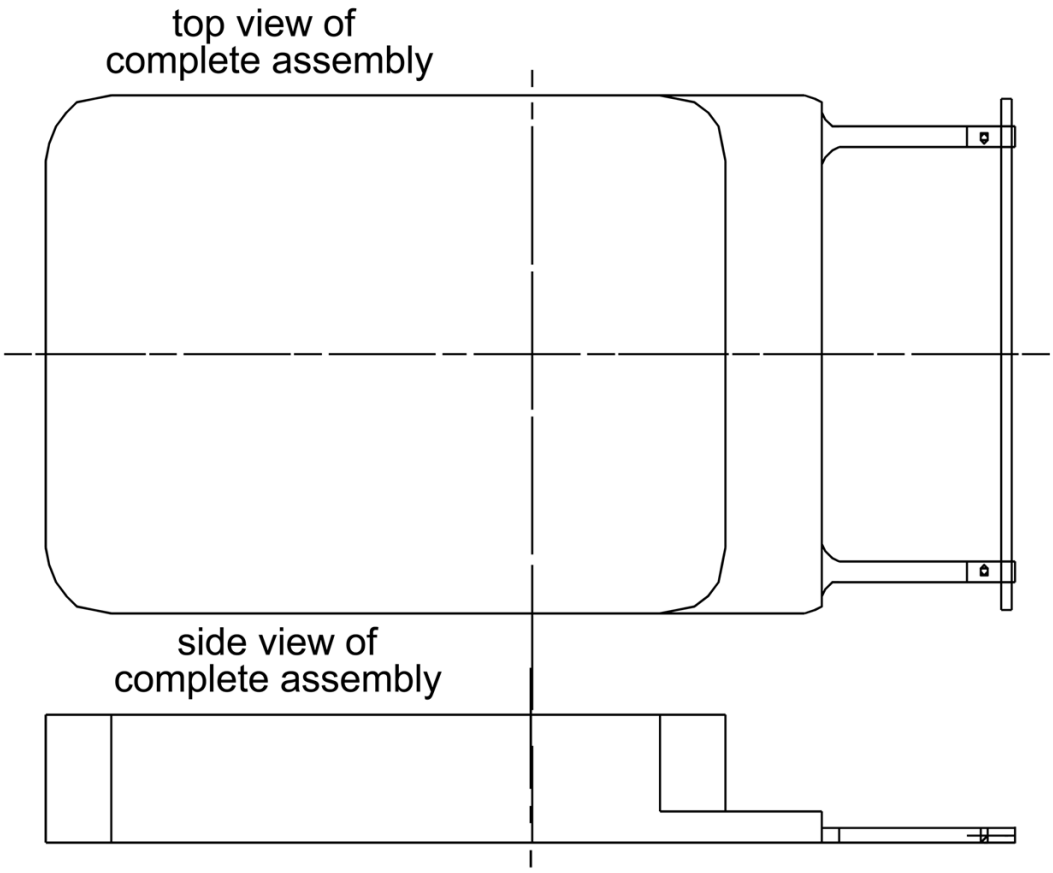

Fig. 2.
Top view and side view of complete assembly for holding 0.2 × 2.0 × 100 mm microslide (VitroCom, Cat. # 3520-100). See companion photographs in Fig. 1n and 1o.

NIH-PA Author Manuscript

NIH-PA Author Manuscript

NIH-PA Author Manuscript

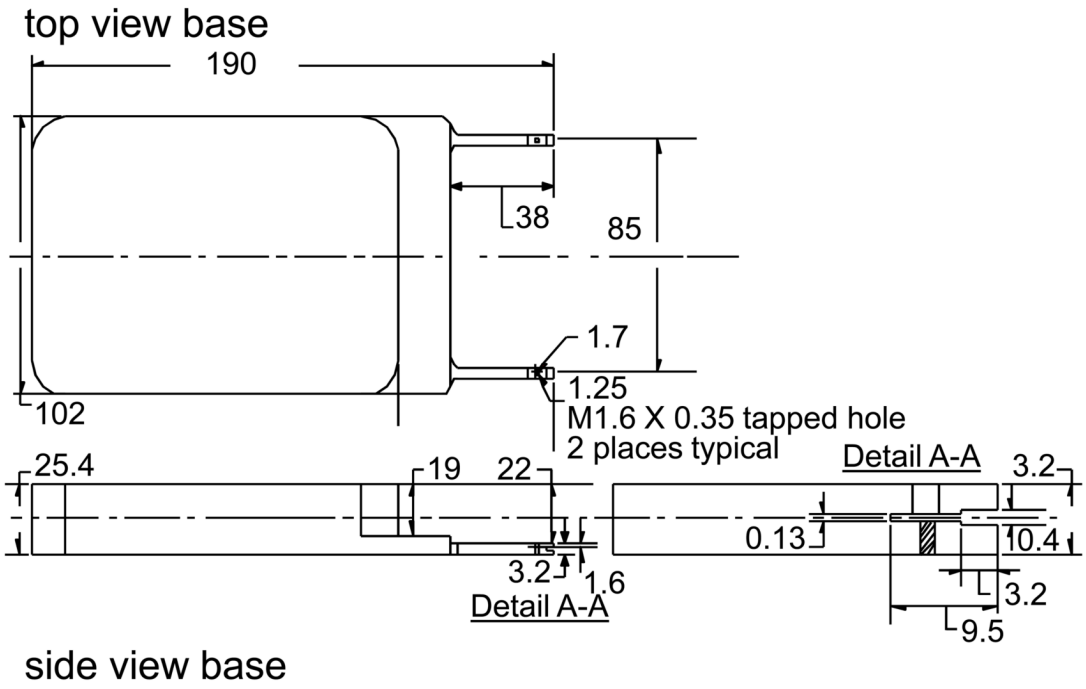

Fig. 3.

Top view, side view and expanded detailed view of complete assembly for holding microslide with measurements in mm. See companion photographs in Fig. 1n and 1o. The Detail A-A section has an expanded view of the two slots in the two prongs that hold the 0.1 mm × 2 mm × 100 mm rectangular glass microslide parallel to the surface of the microscope stage for flat imaging by the upright objective.

NIH-PA Author Manuscript

NIH-PA Author Manuscript

NIH-PA Author Manuscript

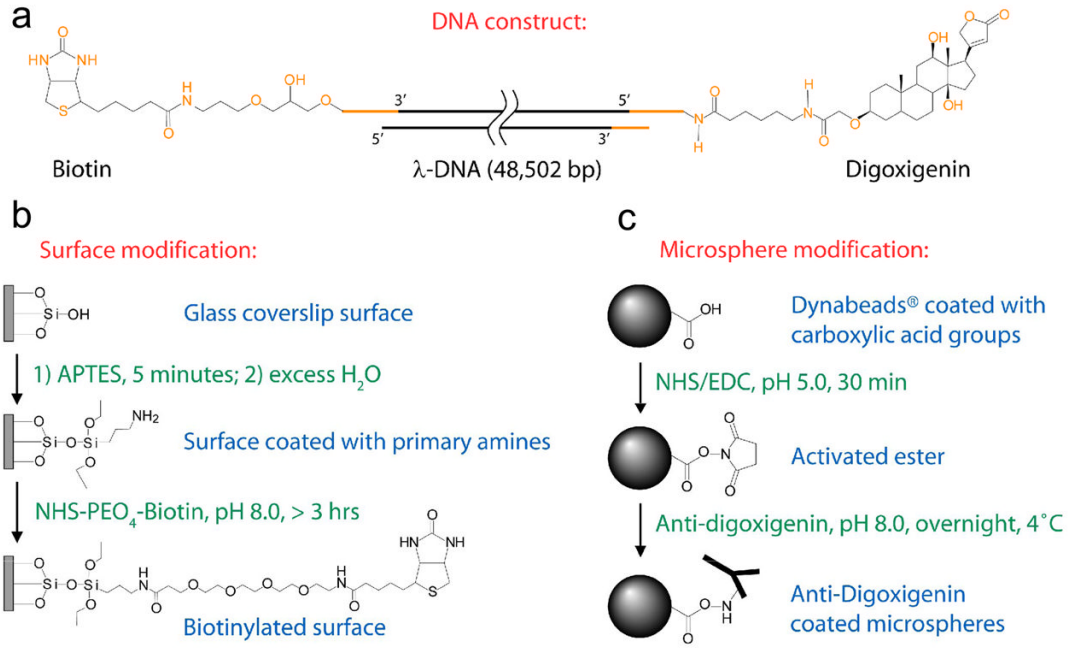

Fig. 4.

DNA attachment to a surface chemistry schematics. (a) Schematic of DNA construct. (b) Schematic of surface modification chemistry. (c) Schematic of microsphere modification.

NIH-PA Author Manuscript

NIH-PA Author Manuscript

NIH-PA Author Manuscript

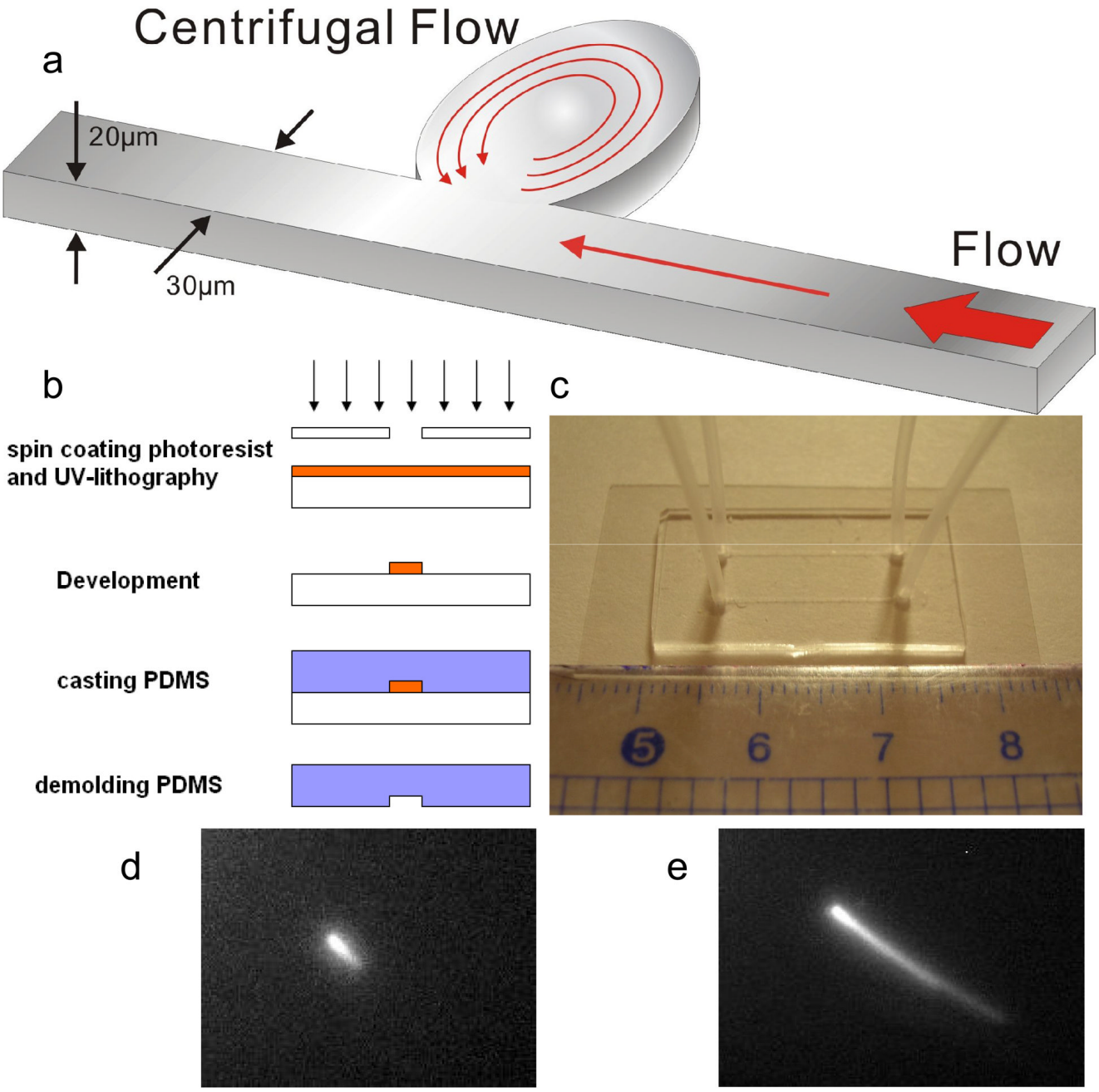

Fig. 5.

The pressure-driven microvortex design for application of high radial acceleration on individual DNA molecules. (a) Schematic of the microfluidic configuration used to create the microvortex. The surface of the glass substrate at the bottom of this microvortex system was treated with anti-digoxigenin for at least one hour to allow the attachment of DNA molecules to the surface of the glass. (b) The process of the soft lithography for fabricating this microvortex system with poly(dimethylsiloxane). (c) An optical image of the poly (dimethylsiloxane) microfluidic device. Fluorescent images of YOYO-1 labeled DNA molecules (d) without and (e) with pressure applied to microvortex system. Scale bar=4 μm.

NIH-PA Author Manuscript

NIH-PA Author Manuscript

NIH-PA Author Manuscript

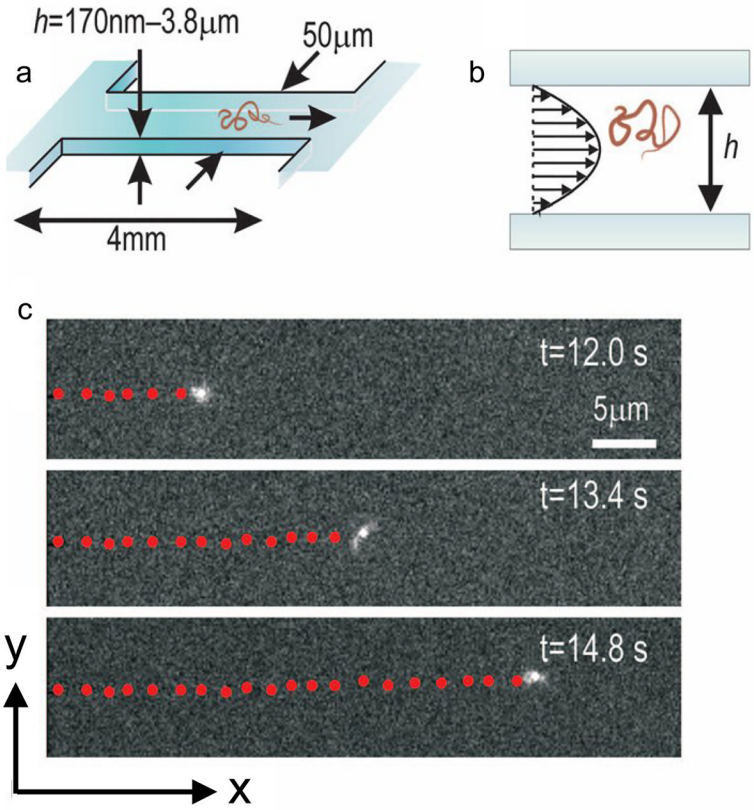

Fig. 6.

Observation of pressure-driven DNA transport in microfluidic and nanofluidic channels. Schematic of a rectangular, 50-μm-wide, 4-mm-long silica fluidic channel (a) and the channel cross-section over which an applied pressure gradient generated a parabolic fluid velocity profile (b). (c) Imaging a fluorescently labeled 48.5-kbp DNA molecule as it was transported through a 250 nm high channel using an applied pressure gradient of 1.44×10^5 Pa/m. The red dots indicate the center-of-mass positions, which were recorded at a rate of 5 Hz [21].

NIH-PA Author Manuscript

NIH-PA Author Manuscript

NIH-PA Author Manuscript

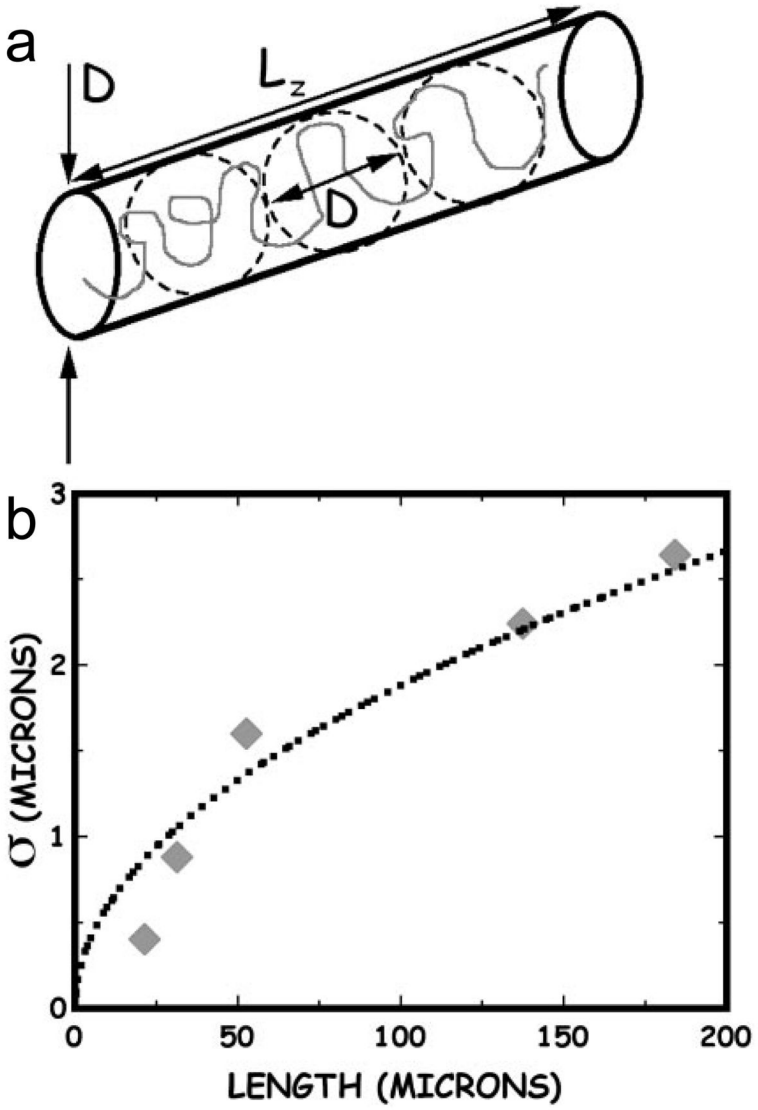

Fig. 7.

Probing fundamental DNA relationships with nanochannels. (a) When a DNA polymer is confined to a nanochannel of diameter D, the polymer must elongate to with a constrained end-to-end distance. (b) Using this approach, the observed standard deviation was determined based on the length of the molecule in a confined channel with a width of 100 nm [22].

NIH-PA Author Manuscript

NIH-PA Author Manuscript

NIH-PA Author Manuscript

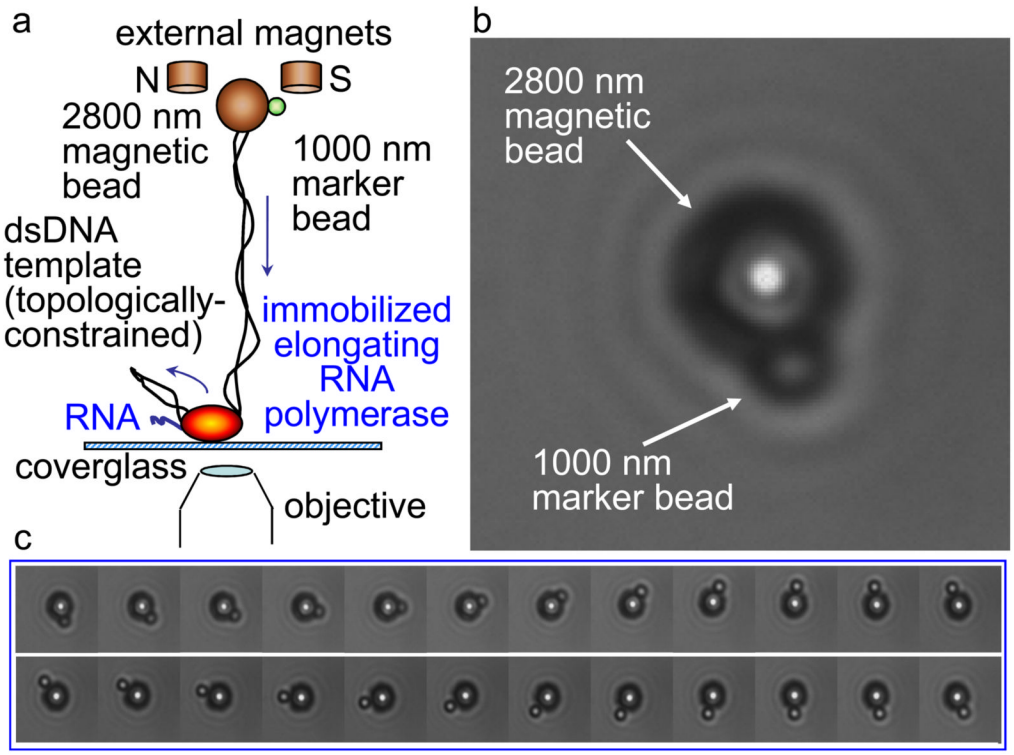

Fig. 8.

Magnetic tweezers used to follow single molecule transcription. (a) Schematic of setup. A double-stranded DNA molecule is tethered between a surface attached molecule of T7 RNA polymerase and a 2.8 μm superparamagnetic bead that is decorated with a 1 μm marker bead. (b) Video image of the 2.8 μm superparamagnetic bead decorated with a 1 μm marker bead. (c) Time lapse images from a movie demonstrating one complete rotation of the marker bead around the superparamagnetic bead. Figure adapted from Pomerantz et al. [24].

NIH-PA Author Manuscript

NIH-PA Author Manuscript

NIH-PA Author Manuscript

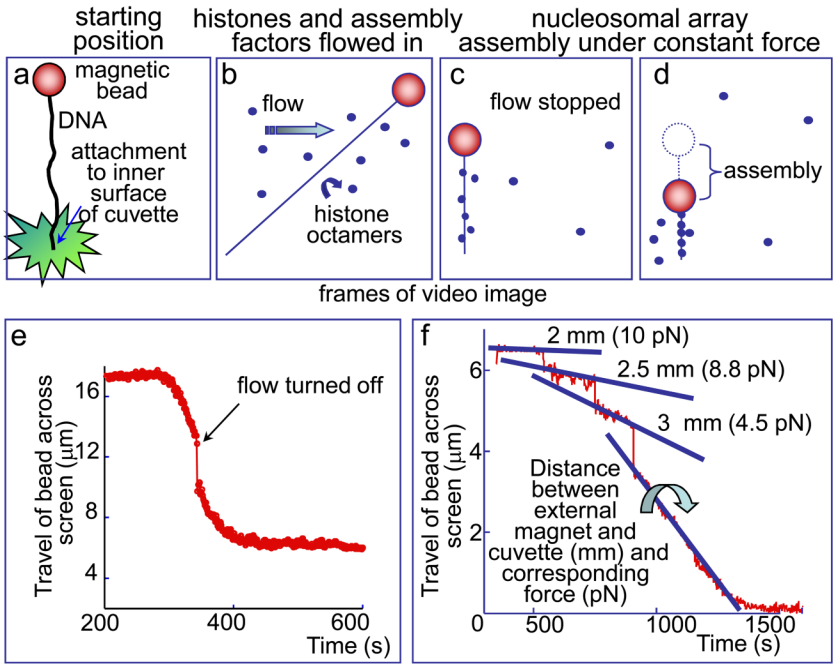

Fig. 9.

Magnetic tweezers using to follow chromatin fiber assembly and disassembly. (a) Schematic of an image of video of the attachment of a single linear DNA molecule tethered between the inner surface of a glass cuvette and a superparamagnetic bead. In the actual video, only the tethered superparamagnetic bead is observed. (b) Schematic of an image of video after flow is introduced. The superparamagnetic bead that was in the upper left hand portion of the image in (a) has now been forced by the left to right flow to be in the upper right hand corner of this image. Additionally, the flow introduces a histone chaperones and core histone octamers, which begin to assemble on the naked DNA molecule and subsequently reduce its overall tether length resulting in the travel of the superparamagnetic bead across the screen and against the direction of the flow. (c) Upon observation that the superparamagnetic bead is traveling across the screen, the flow is stopped and only the external magnet exerts force on the tethered DNA molecule. (d) The flow is off and the observed travel of the bead is only due to assembly caused reduction in the tether length of the DNA molecule as a function of the force exerted by the magnetic field of the external magnet on the superparamagnetic bead. (e) Graph of tracking the center of the superparamagnetic bead over time. After observing the bead traveling across the video screen, we turned off the flow, which results in a precipitous drop in tether length as marked on the graph. Video frame rate 1 per sec. (f) Graph of travel of the bead across the screen as a function of the force on the superparamagnetic bead exerted by the external magnet. Having the external magnet at 2 mm away results in a 10 pN force, which prevents changes in the DNA, tether length and chromatin assembly. Moving the external magnet away using a manual linear caliper weakens the magnetic field exerted on the superparamagnetic bead and results in faster and faster chromatin assembly. Adapted from Leuba et al. [8].

NIH-PA Author Manuscript

NIH-PA Author Manuscript

NIH-PA Author Manuscript

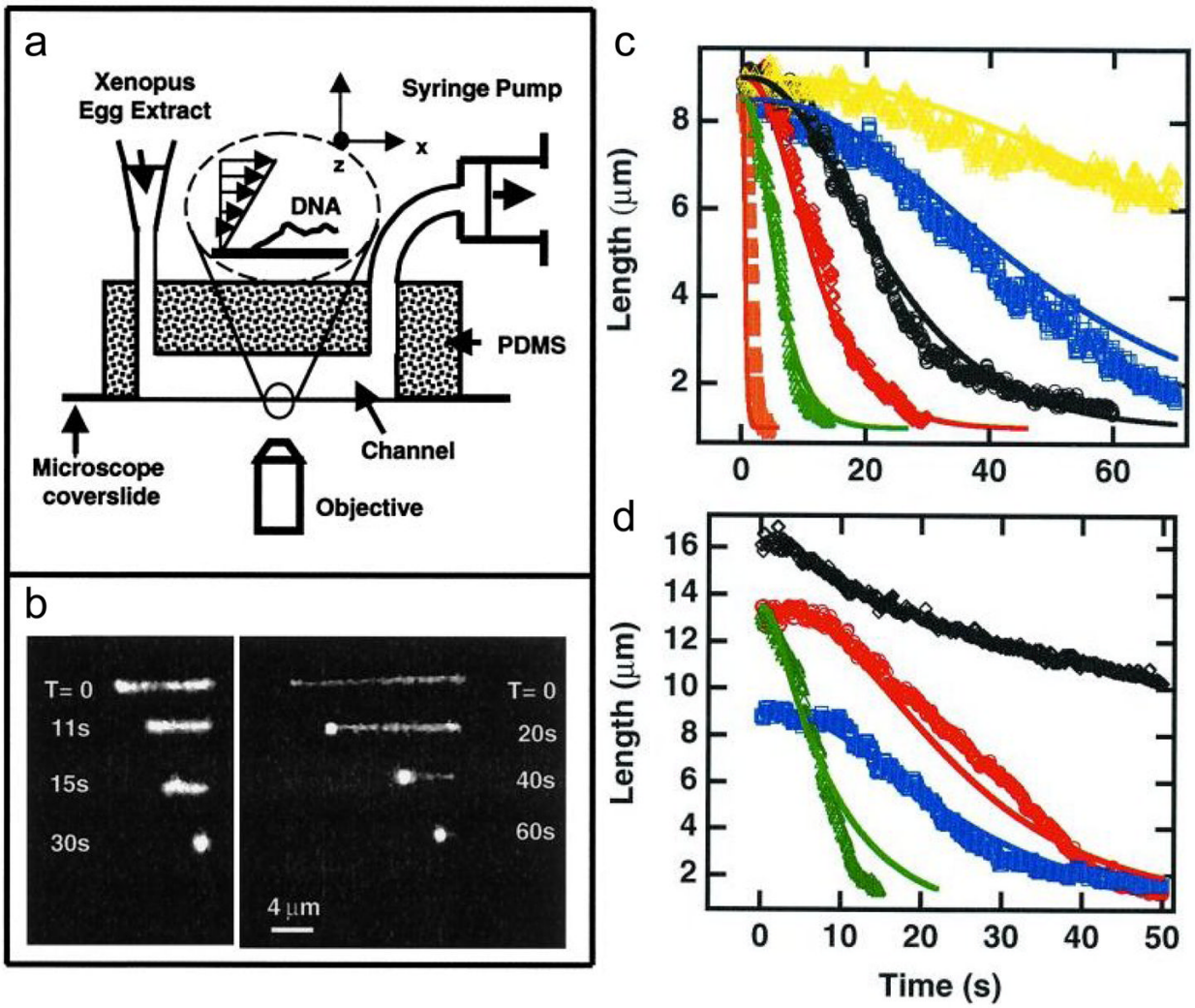

Fig. 10.

Chromatin assembly by flow in a microfluidic chamber. (a) Schematic of a PDMS-fabricated flow chamber. λ-DNA is tethered to a surface and a syringe pump creates flows containing a *Xenopus* egg extract to assemble the DNA molecule into chromatin. (b) Video images of a single fluorescently labeled λ-DNA molecule undergoing assembly at shear rates of 26 s^{-1} (left panel) and 1050 s^{-1} (right panel). (c) Chromatin assembly at a constant shear rate of 26 s^{-1} as a function egg extract dilution ranging from 1:2.5 (far left orange curve) to a much diluted 1:400 (far right yellow curve). (d) Assembly of chromatin in the presence of the 1:100-diluted egg extract as a function of shear rates ranging from 26 s^{-1} (lowest blue curve) to 1050 s^{-1} (highest black curve). The furthest left green curve is chromatin assembly at shear rate with extracts with a ten-fold addition of H2A/H2B. Data from Ladoux et al. [26].